Andreev current in finite-size carbon nanotubes

Smitha Vishveshwara,[1] Cristina Bena,[1] Leon Balents,[1] and Matthew P. A. Fisher[2]
[1]*Department of Physics, University of California, Santa Barbara, California 93106*
[2]*Institute for Theoretical Physics, University of California, Santa Barbara, California 93106-4030*
(Received 22 June 2002; published 23 October 2002)

We investigate the effect of interactions on Andreev current at a normal-superconductor junction when the normal phase is a Luttinger liquid with repulsive interactions. In particular, we study the system of a finite-size carbon nanotube placed between one metallic and one superconducting lead. We show that interactions and finite-size effects give rise to significant deviations from the standard picture of Andreev current at a normal-superconductor junction in the nearly perfect Andreev limit.

DOI: 10.1103/PhysRevB.66.165411 PACS number(s): 73.63.Fg, 71.10.Pm, 74.80.Fp

In recent years, the behavior of superconductors (SC) in contact with Luttinger liquids (LLs) has commanded attention in both theory[1,2] and experiment.[3,4] Josephson junctions made by sandwiching a Luttinger liquid between two superconductors have led to intriguing results such as critical currents orders of magnitude larger than expected.[3] Experimental study of Andreev physics at a niobium superconductor–carbon nanotube junction[4] has yielded significant deviation at low temperatures from the standard picture of Andreev current in a noninteracting one-dimensional electron gas–superconductor junction.[5] As it has been predicted[6] and shown[7] that single-walled metallic carbon nanotubes (NT) exhibit Luttinger liquid behavior, systematic analyses of any setup involving their electronic properties would require taking into account the effect of interactions.

Here we study the Andreev physics[8] in a SC–NT–metallic lead junction, focusing on the effects of the strong repulsive interactions and of the finite size of the nanotube. We focus on energy scales well below the energy gap Δ of the superconductor. Thus, throughout the energy range of interest (i.e., for all the values of temperature or of the applied voltages we consider), the only excitations allowed to exit or enter the superconductor are Cooper pairs and not single electrons. In particular, we focus on the limit of almost perfect Andreev reflection at the SC-NT interface (i.e., very low normal backscattering). We also assume that the nanotube-metal contact is ideal and that the nanotube continues adiabatically into the metallic lead. Under these assumptions we study how a small amount of backscattering at the SC-NT interface would influence the electrical properties of the junction, in particular, the behavior of the conductance.

The treatment we use to obtain the value of the current as a function of the applied voltage is a nonequilibrium Keldysh technique, perturbative in the bare backscattering strength u.[9,11] Characteristic of Luttinger liquids, the amount of backscattering can strongly increase when the energy at which the system is probed decreases. Hence, perturbation theory holds good only above an energy scale $E_c \approx \epsilon_0 (u/\epsilon_0)^{2/(1-g)}$, where g measures the interaction strength ($g=1$ in the absence of interactions). For metallic nanotubes $\epsilon_0 \approx 1$ eV is the subband spacing,[6] and $g \approx 0.25$,[6,7] corresponding to strong repulsive interactions. In the setup considered here, the effect of the finite length L of the nanotube becomes important below the finite-size energy scale $\hbar v/L$. Here, $v = v_F/g$ is the velocity of the charge-carrying quasiparticles in the nanotube, where $v_F \approx 10^6$ m/s is the Fermi velocity. Effects of finite size can be captured in the perturbative approach, as done here, provided $\hbar v/L \gg E_c$.

To summarize our results, a numerical analysis reveals that at zero temperature, the conductance shows a marked drop with decreasing voltage as a consequence of LL physics, consistent with renormalization-group arguments similar to the ones derived in Ref. 2. At voltages much smaller than the finite-size energy $\hbar v/L$, the conductance levels off to a constant. In addition, it exhibits small spikes with a voltage spacing of $\pi \hbar v/2L$ (about 2–3 meV for a nanotube of micron length), reminiscent of resonance peaks from quasi-bound states for charge carriers confined within the length of the tube.

We now present the explicit calculation yielding the conductance as a function of applied voltage for the SC-NT-metal system described above. The s wave SC lies in the region $x<0$ and we assume it to be ideally contacted to a finite-size nanotube of length L in the region $0<x<L$ which continues adiabatically into a metallic lead for $x>L$. We model the system in the semi-infinite region $x>0$, as a four channel LL with interaction parameters appropriate for the nanotube up to $x=L$, and appropriate for no interactions for $x>L$. The bosonized Hamiltonian for this system in the absence of any normal backscattering is given by

$$H_0 = \int_0^\infty dx \sum_a v_a(x) \left[\frac{1}{g_a(x)} (\partial_x \theta_a)^2 + g_a(x) (\partial_x \phi_a)^2 \right]. \tag{1}$$

For simplicity, we have set the constants $\hbar = e = k_B = 1$. Note that $a = \rho_\pm, \sigma_\pm$ correspond to the four free sectors of the theory and are obtained by linear transformations from the spin-channel indices ($1\uparrow$, $1\downarrow$, $2\uparrow$, $2\downarrow$).[6] The relation between the bosonic fields $\theta_{i\alpha}$, $\phi_{i\alpha}$ ($i=1/2, \alpha=\uparrow/\downarrow$) and the original chiral right-/left-moving electron fields $\Psi_{iR/L\alpha}$ are expressed through the bosonization procedure via the transformation $\Psi_{iR/L\alpha} \sim e^{i(\phi_{i\alpha} \pm \theta_{i\alpha})}$. In the nanotube region $0<x<L$ where interactions are present in the net charge density $\rho+$, we take $g_{\rho+}(x) = g \approx 0.25$, and $g_{\rho-,\sigma\pm} = 1$. Also, in the noninteracting region $x>L$, we take $g_a(x) = 1$ for all a's. The velocities of the free modes are given by $v_a(x) = v_F/g_a(x)$. The total charge density is $\rho_{\rm tot} = 2\partial_x \theta_{\rho+}/\pi$.

In the almost perfect Andreev limit, the electrons incident from the nanotube side on the SC-NT interface reflect back as holes with opposite spin: $\Psi_{iL\uparrow/\downarrow}(0)=\Psi^{\dagger}_{iR\downarrow/\uparrow}(0)$ and $\Psi_{iR\uparrow/\downarrow}(0)=\Psi^{\dagger}_{iL\downarrow/\uparrow}(0)$, where i refers to the channel indices 1 and 2. In the bosonized language, these boundary conditions become $\phi_{\rho\pm}(0)=0$ and $\theta_{\sigma\pm}(0)=0$.

The weak normal backscattering at the SC-NT junction can be modeled by modifying the Hamiltonian to $H=H_0+H'$, with

$$H'=\frac{u}{8}\sum_{i=1,2}\sum_{\alpha=\uparrow,\downarrow}[\Psi^{\dagger}_{iR\alpha}(0)\Psi_{iL\alpha}(0)+\text{H.c.}]$$
$$=u\cos[\theta_{\rho^+},(0)]\cos[\theta_{\rho-}(0)], \tag{2}$$

where the bosonized form takes into account the Andreev boundary conditions at the SC-NT interface. For simplicity, we choose not to include the backscattering processes where particles can flip their band index since these terms do not give rise to any new physics.

Following Ref. 11, we integrate out the ϕ variables in the action, as well as the entire x-dependence away from $x=0$. The resulting unperturbed imaginary time Euclidean action becomes

$$S^E_0=\frac{1}{\beta}\sum_n\frac{|\omega_n|}{\tilde{g}(\omega_n)}|\theta_{\rho+}(\omega_n)|^2+\frac{1}{\beta}\sum_n|\omega_n||\theta_{\rho-}(\omega_n)|^2, \tag{3}$$

where β is inverse temperature. Here the imaginary time Fourier transforms for all fields "A" are defined in the standard fashion $A(\omega_n)=\int_0^{\beta}d\tau' A(\tau')e^{i\omega_n\tau'}$, $\omega_n=2\pi n/\beta$. The spatial variations of the interaction parameter $g(x)$ and of the velocity $v(x)$ are reflected by the fact that the effective interaction parameter $\tilde{g}(\omega_n)$ is frequency dependent and has the form,

$$\tilde{g}(\omega_n)=\frac{g(1-y)^2}{1-4gy-y^2}\quad\text{with}\quad y=\left(\frac{1-g}{1+g}\right)e^{-|\omega_n\tau|}. \tag{4}$$

Here $\tau=2L/v$ is the time it takes a charge-carrying quasiparticle with velocity v to bounce back and forth between the ends of the tube. The limits $L,\omega_n\to 0$ and $L,\omega_n\to\infty$ retrieve the expected form $\tilde{g}(\omega_n)=1$ and $\tilde{g}(\omega_n)=g$ for a semi-infinite Fermi liquid and a semi-infinite nanotube, respectively.[10]

Along the lines of Ref. 11, we proceed to construct a real time Keldysh action. We introduce $\theta^{\pm}_a$ fields running over forward and backward paths in time. We define $\theta_a=(\theta^+_a+\theta^-_a)/2$ and $\tilde{\theta}_a=\theta^+_a-\theta^-_a$. The resulting action is $S=S_0+S_1+S_2$ where S_0 is the unperturbed action, S_1 describes the effect of the weak backscattering at the SC-NT interface, and S_2 captures the effect of applying a chemical potential difference $V=\partial_t a$. Thus

$$S_0=\int\frac{d\omega}{2\pi}\frac{\omega}{2}\left[\frac{1}{g(\omega)}+\frac{1}{g(-\omega)}\right]\coth\frac{\omega}{2T}|\tilde{\theta}_{\rho+}(\omega)|^2$$
$$+\int\frac{d\omega}{\pi}\frac{\omega}{g(\omega)}\tilde{\theta}_{\rho+}(\omega)\theta_{\rho+}(-\omega)$$
$$+\int\frac{d\omega}{2\pi}\omega\coth\frac{\omega}{2T}|\tilde{\theta}_{\rho-}(\omega)|^2$$
$$+\int\frac{d\omega}{\pi}\omega\tilde{\theta}_{\rho-}(\omega)\theta_{\rho-}(-\omega),$$

$$S_1=iu\int dt\{\cos[\theta^+_{\rho+}(t)]\cos[\theta^+_{\rho-}(t)]$$
$$-\cos[\theta^-_{\rho+}(t)]\cos[\theta^-_{\rho-}(t)]\},$$

$$S_2=\int d\omega\frac{2\omega}{\pi}[a(\omega)\tilde{\theta}_{\rho+}(-\omega)+\eta(\omega)\theta_{\rho+}(-\omega)]. \tag{5}$$

where $g(\omega)$ is the analytically continued version of $\tilde{g}(\omega_n)$ in Eq. (4) with $|\omega_n\tau|$ replaced by $i\omega\tau$. For all fields "A," we have used the real time Fourier transform convention $A(\omega)=\int dt\,A(t)e^{i\omega t}$. The source field η allows for calculation of the current, $I(t)=2\dot{\theta}_{\rho+}(t)/\pi=(i/2\pi)[\delta S/\delta\eta(t)|_{\eta=0}]$. Average quantities may be derived by taking expectation values with respect to the Keldysh generating functional. $Z=\int\mathcal{D}[\theta^+]\mathcal{D}[\theta^-]e^{-S}$.

Using the above Keldysh action, and treating the backscattering to lowest nonvanishing order in perturbation, we find the expectation value of the current to be

$$I=8\frac{e^2}{h}V-I_B, \tag{6}$$

where from here on, we reinsert factors of e, $\hbar$, and k_B. The first term is associated with the constant conductance $G_0=8(e^2/h)$ in the absence of backscattering. As expected, this ideal Andreev conductance of the finite-size nanotube in the presence of a metallic lead is that of a four mode noninteracting one-dimensional electron gas.[1,10] The backscattering current I_B takes the form

$$I_B=\frac{e}{2\pi}\left(\frac{u}{\hbar}\right)^2\int_0^{\infty}dt\sin\left[\frac{2eVt}{\hbar}\right]e^{[\tilde{\tau}(t)-\tilde{\tau}(0)]}\sin[\tilde{R}(t)]. \tag{7}$$

In the above equation, $\tilde{C}(t)=\Sigma_{a=\rho\pm}C_a(t)$ and $\tilde{R}(t)=\Sigma_{a=\rho\pm}[R_a(-t)-R_a(t)]/2$. For each mode, $C_a(t)$ and $R_a(t)$ are the correlation and response functions, respectively, with $C_a(t)=\langle\theta_a(t)\theta_a(0)\rangle_0$ and $R_a(t)=-i\langle\theta_a(t)\tilde{\theta}_a(0)\rangle_0$. Their Fourier transforms are related by the fluctuation-dissipation theorem, $C_a(\omega)=-\coth(\hbar\omega/2k_BT)\text{Im}[R_a(\omega)]$. Here averages are with respect to the unperturbed action, and we have $R_{\rho+}(\omega)=-i\pi g(\omega)/\omega$ and $R_{\rho-}(\omega)=-i\pi/\omega$

We now make a series expansion of $\tilde{g}(\omega_n)$ in Eq. (4), $\tilde{g}(\omega_n)=g\Sigma_n\alpha_n y^n$. When analytically continued, this gives:

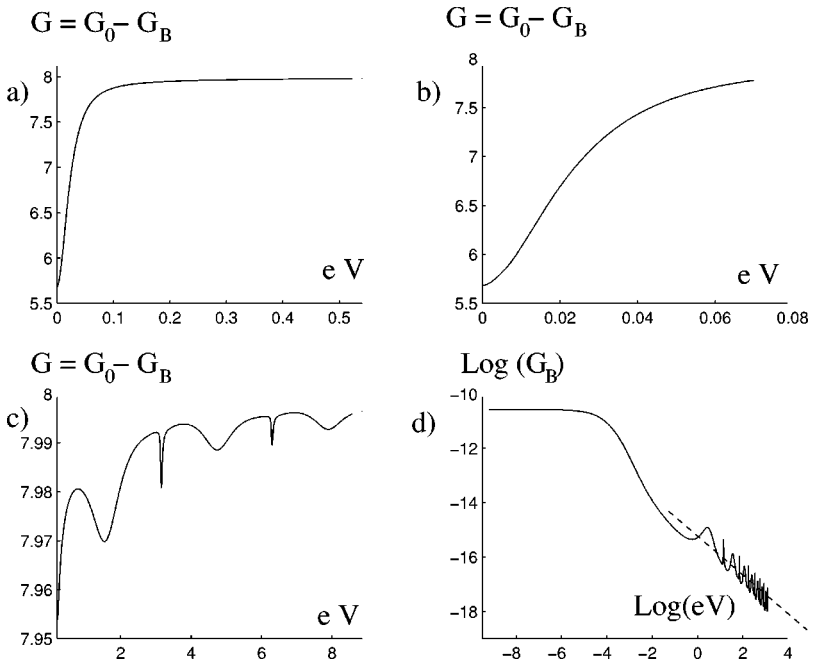

FIG. 1. The net differential conductance $G=dI/dV$ of the nanotube setup in units of e^2/h as a function of applied voltage eV in units of $\hbar/\tau$. The values of the parameters are $g=0.25$, $u=300(\hbar/\tau)$, and $\epsilon_0=10^5(\hbar/\tau)$. (a), (b), and (c) show the conductance for different ranges of applied voltage. The log-log plot of G_B in (d) shows a constant at low voltages and a power law $G_B \sim V^{g-1}$ on average for high voltages, as indicated by the dashed line.

$$g(\omega)=g\sum_{n=0}^{\infty}\alpha_n\left(\frac{1-g}{1+g}\right)^n e^{in\omega\tau}. \tag{8}$$

Substituting the above in Eq. (7) and taking the derivative with respect to the applied voltage gives the following reduction in the conductance due to backscattering $G_B=dI_B/dV$, in the limit $T\to 0$,

$$G_B=2\frac{e^2}{h}\left(\frac{u\tau}{\hbar}\right)^2\sum_{k=0}^{\infty}\sin\left(\pi\sum_{n=0}^{k}\beta_n\right)\int_k^{(k+1)}dx\,x \times\frac{\cos[2eV\tau/\hbar]}{[1+(\epsilon_0 x\tau/\hbar)^2]^{\beta_0}}\prod_{n=1}^{\infty}\left|\left(\frac{x}{n}\right)^2-1\right|^{-\beta_n}, \tag{9}$$

where the coefficients $\beta_n=g(\alpha_n/2)[(1-g)/(1+g)]^n$, for $n>0$, and $\beta_0=(1+g)/2$. We have used the high-energy cutoff ϵ_0 to evaluate the Fourier transforms $C_a(t)$ and $R_a(t)$. Here the terms involving $n\tau$ correspond to physical processes of n bounces of the quasiparticles at the boundaries of the nanotube. Note that besides the weak backscattering at the SC-NT interface, the quasiparticles can also backscatter at the nanotube–metallic lead junction even in the absence of a barrier, solely as a result of the mismatch of the values of the net charge and velocity of the free modes in the nanotube and in the metal.

The most revealing analysis of Eq. (9) comes from numerical evaluation. We restrict the infinite sums of Eq. (9) to a finite number of terms, and introduce an explicit high-energy cutoff ϵ_0, in order to regulate singularities. We ensure that errors coming from both truncations are negligible. In Fig. 1, we plot the net differential conductance $dI/dV=G_0-G_B$, as the one of experimental relevance. The conductance drops with decreasing voltage and levels off at voltages much smaller than $\hbar/\tau$. To see why this might be expected, notice that at large voltages $eV\gg\hbar/\tau$, the time scale at which the system is probed is much shorter than τ, and the conductance roughly behaves as if the nanotube were semi-infinite. Characteristics of Luttinger liquid physics, it thus drops as $G_B\propto u^2(2geV/\epsilon_0)^{g-1}$ on average, as shown in Fig. 1(d). This limiting behavior can be seen directly in Eq. (9) by taking $\tau\to\infty$. At low voltages $eV\ll\hbar/\tau$, the associated time scale is long enough to capture the effect of the metallic lead and of multiple backscattering events at its interface. With decreasing voltage, the conductance ultimately levels off to a constant, as per Ohm's law for the metallic lead. This limit can be obtained in Eq. (9) by setting $\tau=0$.

A striking feature of the plots is the presence of spikes at probe values $eV=n\hbar\pi/\tau$, with "n" being an integer. As their magnitude is minuscule compared to the net variation in conductance, it would be difficult to measure them in experiment. However, these resonances do exist, and are signatures of the quasibound states that one would expect within the nanotube region, given that here the interaction parameter and velocity are different from those of the metallic lead.

As a variation of the above setup, let us now replace the nanotube by a finite-size Luttinger liquid with only two transport channels (spin $\uparrow/\downarrow$). Such a situation can be realized by using, for instance, an etched quantum wire. The corresponding free modes carry net charge ρ and spin σ, and are linear combinations of the two spin species. Andreev boundary conditions at the superconducting junction require $\phi_\rho(0)=0$, $\theta_\sigma(0)=0$ in corresponding bosonized variables. Thus, the system can be effectively described by a single channel in the θ variables. This allows for us to study the particular situation where the velocity of the charge mode in the Luttinger liquid $v=v_F/g$ would equal the Fermi velocity v_F^l in the metallic lead, i.e., $v_F^l=v_F/g$. Hence, we can focus on the physics arising purely from the mismatch of the charge of the elementary excitations in the Luttinger liquid and the lead. This would not have been possible for the case of the nanotube as it is described by two modes moving at different velocities, and matching the velocity of one mode

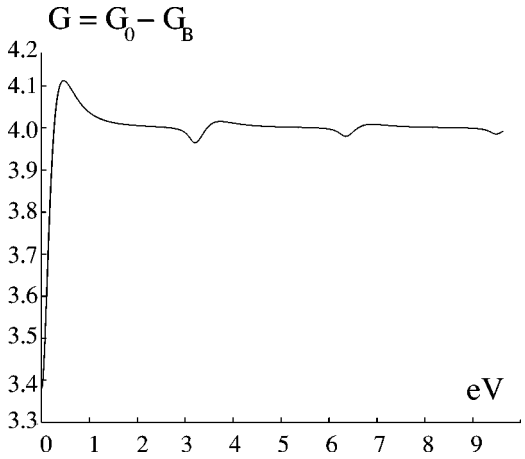

FIG. 2. The net conductance G of the two-mode Luttinger liquid setup in units of e^2/h as a function of applied voltage eV in units of $\hbar/\tau$. The values of the parameters are $g=0.25$, $u=1.4(\hbar/\tau)$ and $\epsilon_0=10^4(\hbar/\tau)$.

to the Fermi velocity of the metallic lead would cause a velocity mismatch in the other mode. We calculate the conductance as a function of applied voltage for this system in a manner completely analogous to the one described above for the nanotube. The major difference here is that we have only one mode with effective interaction parameter

$$\tilde{g}(\omega_n)=\frac{g}{1-(1-g)\exp(-|\omega_n\tau|)}. \tag{10}$$

The resulting conductance is plotted in Fig. 2. The magnitude of the resonances at $eV=n\hbar\pi/\tau$ spans a larger fraction of the net variation in conductance compared to the case of the nanotube. It is noteworthy that these resonances exist in spite of the fact that there is no mismatch of velocities of the free phonon modes in the Luttinger liquid and in the metal. As expected, the phonons rebound at the Luttinger liquid–metal interface solely due to the impedance mismatch in the charge sector.

To summarize, we have looked at how the standard picture for Andreev current through a superconductor–metallic wire junction gets altered in the Andreev limit in the presence of interactions and finite-size effects. The Andreev conductance shows a reduction with decreasing voltage which finally levels off at the lowest voltages. Finite-size effects also give rise to resonances manifest as small spikes in the conductance.

Finally, turning to experiment, while Luttinger liquid behavior in nanotubes contacted to normal leads has been analyzed in great detail,[7] by no means has it been studied systematically in the presence of superconducting leads. As seen here, one would certainly expect Luttinger liquid effects to yield significant deviations from the standard picture of Andreev physics for noninteracting one-dimensional wires. Consistent with our assumptions such experiments can be performed, for example, in superconductor-nanotube junctions, in which the superconducting gap energy is of the order of several meV, while for a nanotube of a few microns, the finite-size energy is in the range of a meV. At temperatures of the order of 100 mK, thermal effects are expected to be negligible. These conditions are well within experimental reach, and systematic analyses of such setups could potentially reveal rich physics arising from bringing Luttinger liquids in contact with superconductors.

This work was supported by NSF grants DMR-9985255, DMR-97-04005, DMR95-28578, PHY94-07194, and the Sloan and Packard foundations.

[1] R. Fazio, F. W. J. Hekking, and A. A. Odintsov, Phys. Rev. Lett. **74**, 1843 (1995); D. L. Maslov, M. Stone, P. M. Goldbart, and D. Loss, Phys. Rev. B **53**, 1548 (1996); Y. Takane, J. Phys. Soc. Jpn. **66**, 537 (1997); R. Fazio, F. W. J. Hekking, A. A. Odintsov, and R. Raimondi, cond-mat/9811217 (unpublished).

[2] I. Affleck, J.-S. Caux, and A. M. Zagoskin, Phys. Rev. B **62**, 1433 (2000).

[3] A. Yu. Kasumov *et al.*, Science **284**, 1508 (1999).

[4] A. F. Morpurgo, J. Kong, C. M. Marcus, and H. Dai, Science **286**, 263 (1999).

[5] G. E. Blonder, M. Tinkham, and T. M. Klapwijk, Phys. Rev. B **25**, 4515 (1982).

[6] C. L. Kane, L. Balents, and M. P. A. Fisher, Phys. Rev. Lett. **79**, 5086 (1997); R. Egger and A. Gogolin, *ibid.* **79**, 5082 (1997).

[7] M. Bockrath *et al.*, Nature (London) **397**, 598 (1999); Z. Yao, H. Postma, L. Balents, and C. Dekker, *ibid.* **402**, 273 (1999); H. Postma, M. de Jonge, Z. Yao, and C. Dekker, cond-mat/0009055 (unpublished).

[8] A. F. Andreev, Zh. Eksp. Teor. Fiz. **46**, 1823 (1964) [JETP **19**, 1228 (1964)]; **49**, 655 (1965) [**49**, 455 (1966)].

[9] L. V. Keldysh, Zh. Eksp. Teor. Fiz. **47** 1515 (1964) [Sov. Phys. JETP **20**, 1018 (1965)]; M. P. A. Fisher and W. Zwerger, Phys. Rev. B **32**, 6190 (1985).

[10] M. P. A. Fisher and L. I. Glazman, in *Mesoscopic Electron Transport*, Vol. 345 of *NATO Advanced Study Institute, Series E: Applied Sciences* edited by L. L. Sohn, L. P. Kouwenhoven, and G. Schon (Kluwer Academic Publishing, Dordrecht, 1997).

[11] C. L. Kane and M. P. A. Fisher, Phys. Rev. Lett. **72**, 724 (1994).